

Parametric instability of oscillations of a vortex ring in a z -periodic Bose-Einstein condensate and the recurrence to starting state

Victor P. Ruban*

L.D. Landau Institute for Theoretical Physics RAS, Moscow, Russia

(Dated: September 20, 2018)

The dynamics of deformations of a quantum vortex ring in a Bose-Einstein condensate with periodic equilibrium density $\rho(z) = 1 - \epsilon \cos z$ has been considered within the local induction approximation. Parametric instabilities of the normal modes with azimuthal numbers $\pm m$ have been revealed at the energy integral E near values $E_m^{(p)} = 2m\sqrt{m^2 - 1}/p$, where p is the resonance order. Numerical simulations have shown that already at $\epsilon \sim 0.03$ a rapid growth of unstable modes with $m = 2$, $p = 1$ to magnitudes of order of unity is typical, which is then followed, after a few large oscillations, by fast return to a weakly excited state. Such behavior corresponds to an integrable Hamiltonian of the form $H \propto \sigma(E_2^{(1)} - E)(|b_+|^2 + |b_-|^2) - \epsilon(b_+b_- + b_+^*b_-^*) + u(|b_+|^4 + |b_-|^4) + w|b_+|^2|b_-|^2$ for two complex envelopes $b_{\pm}(t)$. The results have been compared to parametric instabilities of vortex ring in condensate with density $\rho(z, r) = 1 - r^2 - \alpha z^2$, which take place at $\alpha \approx 8/5$ and at $\alpha \approx 16/7$.

Introduction. The dynamics of quantum vortices in a trapped atomic Bose-Einstein condensate with spatially inhomogeneous equilibrium density $\rho(\mathbf{r})$ differs significantly from their dynamics in a uniform system, and the differences are not only quantitative but also qualitative (see review [1] and references therein). Development of experimental methods in this field makes actual new and diverse profiles $\rho(\mathbf{r})$. Therefore, vortices in nonuniform systems continue to attract interest in experiment as well as in the theory [2–16]. In the general case the problem is quite complicated, because vortices interact with potential excitations and with non-condensate atoms. But if the condensate at zero temperature is in the Thomas-Fermi regime (the vortex core width ξ is much smaller than a typical scale of the inhomogeneity and the vortex size R_*), then one can neglect the potential degrees of freedom and use the “anelastic” hydrodynamic approximation [2–4, 7, 11, 17, 18]. If, besides that, a vortex line configuration is far from self-intersections, then a simple mathematical model is applicable, the local induction equation [2–4]

$$\mathbf{R}_t|_{\text{normal}} = \frac{\Gamma\Lambda}{4\pi} \left(\varkappa \mathbf{b} + [\nabla \ln \rho(\mathbf{R}) \times \boldsymbol{\tau}] \right), \quad (1)$$

where $\mathbf{R}(\beta, t)$ is the geometric shape of the filament depending on arbitrary longitudinal parameter β and time t , the parameter $\Gamma = 2\pi\hbar/m_{\text{atom}}$ is the velocity circulation quantum, $\Lambda = \ln(R_*/\xi) \approx \text{const}$ is a large logarithm, \varkappa is a local curvature of the vortex line, \mathbf{b} is the unit binormal vector, and $\boldsymbol{\tau}$ is the unit tangent vector. To make formulas clean, below we use dimensionless quantities, so that $\Gamma\Lambda/4\pi = 1$, $R_* \sim 1$. It is a well known fact that in the case $\rho = \text{const}$, the local induction equation is reduced by the Hasimoto transform [19] to the one-dimensional (1D) focusing nonlinear Schrödinger equation, so the vortex line dynamics against a uniform

background is nearly integrable. For nonuniform density profiles investigation of this model is still in the very beginning [13, 14, 20, 21]. Even the simplest 1D-periodic density profile

$$\rho(z) = 1 - \epsilon \cos z \quad (2)$$

was not applied so far in the framework of Eq.(1), although, by the way it is easily realized in optical traps. The purpose of this work is to fill this gap in the theory by considering the propagation of a deformed quantum vortex ring through Bose-Einstein condensate with nonuniform density (2). By theoretical analysis and numerical simulations we shall identify here such interesting phenomena as parametric resonance and a quasi-recurrence to a weakly excited starting state. To the best author’s knowledge, an idea about possibility of these effects in the system under consideration was not put forward previously by anyone. Besides that, we will compare the results with other type parametric instabilities of a vortex ring, which were found in recent studies to take place in harmonically trapped condensate with parabolic density profile $\rho_h(z, r) = 1 - r^2 - \alpha z^2$ near two definite values of the anisotropy parameter $\alpha^{(1)} = 8/5$ and $\alpha^{(2)} = 16/7$.

Variational structure of equations. For our purposes it will be convenient to take angle φ in the cylindrical coordinate system as the longitudinal parameter, while the two other coordinates will be considered as unknown functions $R(\varphi, t)$ and $Z(\varphi, t)$ (apparently, both 2π -periodic on φ) which determine geometric shape of the vortex ring at an arbitrary time moment. We restrict our study by axisymmetric density profiles $\rho(z, r)$. Equations of motion for $R(\varphi, t)$ and $Z(\varphi, t)$, equivalent to the vector equation (1), can be then written in a non-canonical Hamiltonian form,

$$\begin{aligned} \rho(Z, R)R\dot{Z} = & -\frac{\partial}{\partial\varphi} \frac{\rho(Z, R)R'}{\sqrt{R^2 + R'^2 + Z'^2}} \\ & + \frac{\partial\rho(Z, R)}{\partial R} \sqrt{R^2 + R'^2 + Z'^2} + \frac{\rho(Z, R)R}{\sqrt{R^2 + R'^2 + Z'^2}} \end{aligned} \quad (3)$$

*Electronic address: ruban@itp.ac.ru

$$-\rho(Z, R)R\dot{R} = -\frac{\partial}{\partial\varphi} \frac{\rho(Z, R)Z'}{\sqrt{R^2 + R'^2 + Z'^2}} + \frac{\partial\rho(Z, R)}{\partial Z} \sqrt{R^2 + R'^2 + Z'^2}, \quad (4)$$

where primes denote the partial derivatives on φ , and dots stand for time derivatives. The corresponding Lagrangian has the following form

$$\mathcal{L} = \int F(Z, R)\dot{Z}d\varphi - \int \rho(Z, R)\sqrt{R^2 + R'^2 + Z'^2}d\varphi, \quad (5)$$

where it is implied that for $\rho(z, r) = f(z, r^2/2)$ the function $F(Z, R)$ is determined by formula

$$F(Z, R) = \int_{U(z)}^{R^2/2} f(Z, u)du, \quad (6)$$

and $U(z)$ can be chosen arbitrary. In particular, for r -independent density profiles $\rho(z)$ we obtain $F = \rho(Z)R^2/2$, while for condensate in a harmonic trap it is convenient to take $F = -(1 - R^2 - \alpha Z^2)^2/4 = -\rho_h^2/4$.

Parametric instability. Let us first consider the case $\rho = \rho(z)$, when unperturbed propagation of a perfectly circular ring along z axis is described by solutions of the form $R = R_0(t)$ and $Z = Z_0(t)$, which satisfy a simple system of ordinary differential equations

$$\dot{Z}_0 = 1/R_0, \quad \dot{R}_0 = -\rho'(Z_0)/\rho(Z_0). \quad (7)$$

Obviously, this system has integral of motion $R_0\rho(Z_0) = E = \text{const}$. Let us consider now the dynamics of small azimuthal deviations from the perfect shape, by writing

$$R = R_0(t) + \sum_{m \geq 1} [R_m e^{im\varphi} + R_m^* e^{-im\varphi}], \quad (8)$$

$$Z = Z_0(t) + \sum_{m \geq 1} [Z_m e^{im\varphi} + Z_m^* e^{-im\varphi}], \quad (9)$$

where $R_m(t)$ and $Z_m(t)$ are small complex Fourier coefficients. A linearized system for them follows from Eqs.(3)-(4). With taking into account the relation $d/dt = (1/R_0)d/dZ_0$ and the presence of integral of motion $R_0\rho(Z_0) = E$, we easily obtain

$$\frac{d}{dZ_0} Z_m = \frac{\rho(Z_0)}{E} [m^2 - 1] R_m, \quad (10)$$

$$-\frac{d}{dZ_0} R_m = \frac{\rho(Z_0)}{E} \left[m^2 + \frac{E^2}{\rho^2(Z_0)} \left(\frac{\rho'(Z_0)}{\rho(Z_0)} \right)' \right] Z_m \quad (11)$$

It is convenient to introduce here instead of Z_0 a new independent variable μ in accordance with $\rho(Z_0)dZ_0 = d\mu$. Then the linearized system looks very simple:

$$\frac{dZ_m}{d\mu} = \frac{1}{E} [m^2 - 1] R_m, \quad (12)$$

$$-\frac{dR_m}{d\mu} = \frac{1}{E} \left[m^2 + \frac{E^2}{f(\mu)} \frac{d^2 f(\mu)}{d\mu^2} \right] Z_m, \quad (13)$$

where function $f(\mu) = \rho(Z_0(\mu))$ has been introduced. In our case this dependence is 2π -periodic, so after reduction of (12)-(13) to a single differential equation of the second order we obtain a Hill equation,

$$\frac{d^2 Z_m}{d\mu^2} + \left[\frac{m^2(m^2 - 1)}{E^2} + (m^2 - 1) \frac{f''(\mu)}{f(\mu)} \right] Z_m = 0, \quad (14)$$

which is widely known as the main mathematical model describing parametric resonance in linear systems. From here conditions for parametric resonance of order $p = 1, 2, \dots$ immediately follow: $E \approx E_m^{(p)} = 2m\sqrt{m^2 - 1}/p$. In this work we mainly concentrate on the case $m = 2$, $p = 1$. Let us note that at small values of the density modulation depth $\epsilon \ll 1$ we have approximately $f''(\mu)/f(\mu) \approx \epsilon \cos \mu$, i.e. the Hill equation takes form of the Mathieu equation. At the same time, the modulation depth of the nonuniform coefficient in Eq.(14) is equal to 12ϵ . The spatial increment of the instability at exact resonance is given, as can be easily shown, by formula $\gamma^{(z)} \approx (3/2)\epsilon$. It corresponds to the growth of the elliptic mode of the ring by a factor of $\exp(3\pi\epsilon)$ per one period of the density modulation. Even with relatively small $\epsilon \sim 0.03$ we thus have a very rapid growth of deviations.

Numerical simulations. In order to investigate a nonlinear stage of the parametric instability development, solutions of the evolutionary system (3)-(4) at $\rho = 1 - \epsilon \cos z$ with different initial conditions were found numerically by a pseudo-spectral method using a Runge-Kutta 4-th order procedure for the time stepping. Since it follows from the linear analysis of perturbations that at small ϵ near parametric resonance the dependencies $R_2(Z_0)$ and $Z_2(Z_0)$ have an oscillating character with period near 4π , while their linear combinations $[R_2 - i(2/\sqrt{3})Z_2]$ and $[R_2^* - i(2/\sqrt{3})Z_2^*]$ are mainly proportional to $\exp(-iZ_0/2)$ (when higher harmonics are neglected), then for better understanding of the system dynamics it is useful to study behaviour of ‘‘slow’’ complex-valued functions

$$A_c = +2[\text{Re}(R_2) - i(2/\sqrt{3})\text{Re}(Z_2)] \exp(iZ_0/2), \quad (15)$$

$$A_s = -2[\text{Im}(R_2) - i(2/\sqrt{3})\text{Im}(Z_2)] \exp(iZ_0/2). \quad (16)$$

Let us note that A_c and A_s are complex envelopes for the amplitudes of standing modes $\cos 2\varphi$ and $\sin 2\varphi$ respectively, while $A_{\pm} = (A_c \mp iA_s)/2$ correspond to decomposition of elliptic perturbations of the vortex ring on the propagating modes $\exp(\pm 2i\varphi)$.

Two typical numerical examples of the ring perturbation dynamics are presented in Fig.1. The main features there which catch our eye are the periodic synchronous returns of the system to a weakly excited state, alternating with strongly deformed ring configurations, the last ones having different angular orientation on the (x, y) plane. Therefore, periodic is not each envelope taken separately, but their combination $\sqrt{|A_c|^2 + |A_s|^2}$ which is independent on angle reading. Only with increase of

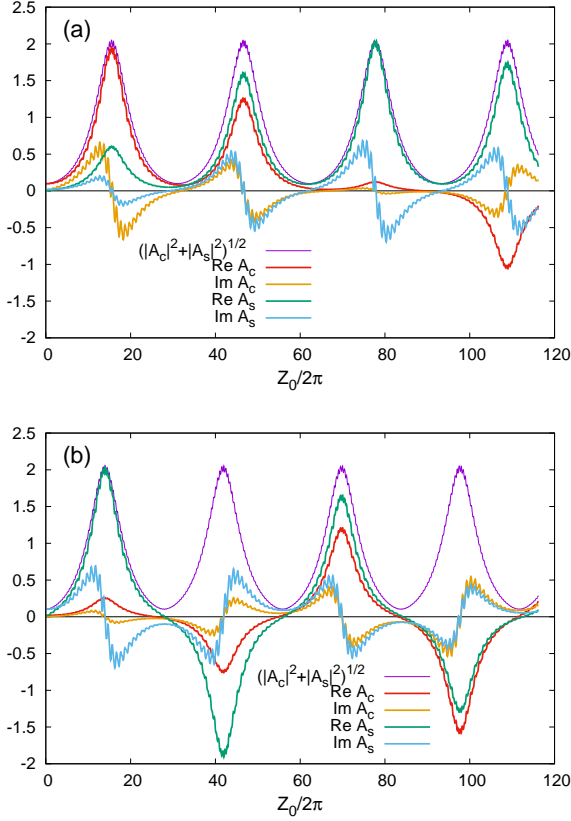


FIG. 1: Two examples of the vortex ring parametric instability development and its return to a weakly excited state at $\epsilon = 0.03$. The residual oscillations on the curves are caused by the presence of higher harmonics, which are typical for parametrically unstable systems. Initial conditions in case (a): $R(0) = 4\sqrt{3} + 0.10 \cos(2\varphi)$, $Z(0) = -0.02(\sqrt{3}/2) \sin(2\varphi)$, it corresponds to $A_c(0) = 0.10$, $A_s(0) = 0.02i$; in case (b): $R(0) = 4\sqrt{3} + 0.02 \cos(2\varphi)$, $Z(0) = -0.10(\sqrt{3}/2) \sin(2\varphi)$, it corresponds to $A_c(0) = 0.02$, $A_s(0) = 0.10i$.

the parameter ϵ to values $\epsilon \sim 0.1$, the regular behaviour is destructed (not shown in the figures).

Such a recurrent dynamics is typical of autonomic integrable systems with a few degrees of freedom. Therefore it makes sense to derive a simplified model which could reproduce at least semi-quantitatively the dependencies observed in the numerical experiment.

Explanation of the recurrence phenomenon. In order to explain theoretically the recurrent dynamics of ring deformations, we introduce new canonically conjugate variables

$$S = \frac{R^2}{2} \rho^2(Z) = S_0 + \sum_{m \geq 1} [S_m e^{im\varphi} + S_m^* e^{-im\varphi}], \quad (17)$$

$$\chi = \int_0^Z \frac{dz}{\rho(z)} = \chi_0 + \sum_{m \geq 1} [\chi_m e^{im\varphi} + \chi_m^* e^{-im\varphi}], \quad (18)$$

and expand on small disturbances the corresponding Hamiltonian of the ring,

$$H = \int \sqrt{2S + g^4(\chi) \chi'^2 + g^2(\chi) \left(\frac{\sqrt{2S}}{g(\chi)} \right)^2} d\varphi, \quad (19)$$

with $g(\chi(z)) = \rho(z)$ [at small ϵ we have $g(\chi) = 1 - \epsilon \cos(\chi) + \mathcal{O}(\epsilon^2)$]. At that we obtain $H/(2\pi) = H^{\{0\}} + \sum_{m \geq 1} H_m^{\{2\}} + H^{\{3\}} + H^{\{4\}} \dots$, where $H^{\{0\}} = \sqrt{2S_0}$,

$$H_m^{\{2\}} = -\frac{|S_m|^2}{\sqrt{(2S_0)^3}} + \frac{m^2}{\sqrt{2S_0}} \left[g_0^4 |\chi_m|^2 + \frac{|S_m|^2}{2S_0} - \frac{g_0'}{g_0} (S_m \chi_m^* + S_m^* \chi_m) + \frac{2S_0 g_0'^2}{g_0^2} |\chi_m|^2 \right] \quad (20)$$

and $g_0 = g(\chi_0)$. Let us separate in $H_m^{\{2\}}$ the terms of zeroth order on ϵ and in a standard way construct on them the normal complex variables

$$a_m = \frac{\sqrt{m^2 - 1} (2S_0)^{-3/4} S_m - im (2S_0)^{-1/4} \chi_m}{\sqrt{2\omega_m}}, \quad (21)$$

$$a_{-m} = \frac{\sqrt{m^2 - 1} (2S_0)^{-3/4} S_m^* - im (2S_0)^{-1/4} \chi_m^*}{\sqrt{2\omega_m}}, \quad (22)$$

where the frequency in spatially uniform system is

$$\omega_m = \frac{m\sqrt{m^2 - 1}}{2S_0}. \quad (23)$$

The variable χ_0 is slightly renormalized at that, but we keep the same notation.

It is very important that at $\epsilon = 0$ our system is completely integrable. Therefore there exist such renormalized normal variables $b_m = a_m + \mathcal{O}\{a^2\}$, that three-wave interactions are excluded, while fourth-order terms have the form $\tilde{H}^{\{4\}} = (1/2) \sum_{k,n} W_{kn} |b_k|^2 |b_n|^2$.

Let us consider mode excitations for resonance number m at $p = 1$ and introduce slow envelopes for the corresponding normal variables:

$$b_m = b_+ \exp(-i\chi_0/2), \quad b_{-m} = b_- \exp(-i\chi_0/2). \quad (24)$$

After that we average $\tilde{H}_m^{\{2\}}$ on the density oscillations with an accuracy up to the first order on ϵ . Non-trivial averaging is required for the term proportional to $-4\epsilon \cos(\chi_0) |\chi_m|^2$, and also for $-\epsilon \sin(\chi_0) (S_m \chi_m^* + S_m^* \chi_m)$. As the result of substitution (24) and subsequent averaging, an effective Lagrangian takes the following form:

$$L \approx S_0 \dot{\chi}_0 + i\dot{b}_+ b_+^* + i\dot{b}_- b_-^* + \frac{\dot{\chi}_0}{2} (|b_+|^2 + |b_-|^2) - \sqrt{2S_0} - \frac{m\sqrt{m^2 - 1}}{2S_0} (|b_+|^2 + |b_-|^2) + \epsilon \frac{\sqrt{m^2 - 1}}{4m} (b_+ b_- + b_+^* b_-^*) - T(|b_+|^4 + |b_-|^4) - W|b_+|^2 |b_-|^2. \quad (25)$$

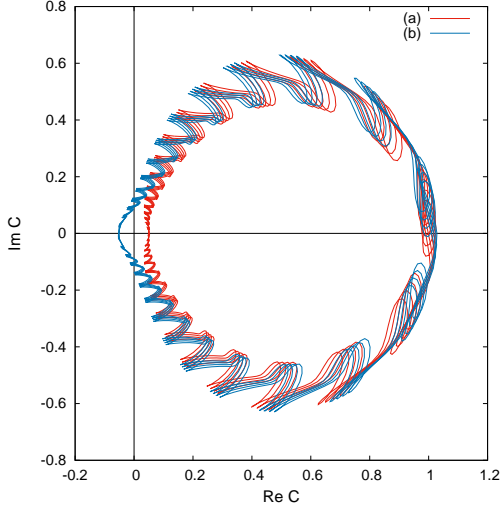


FIG. 2: Quasi-closed phase trajectories in plane C , corresponding to two numerical experiments presented in Fig.1.

It is important that we have here an integrable Hamiltonian system with three degrees of freedom. Apparent integrals of motion, besides the Hamiltonian itself, are

$$S_0 + \frac{1}{2}(|b_+|^2 + |b_-|^2) = I = \text{const}, \quad (26)$$

$$|b_+|^2 - |b_-|^2 = D = \text{const}. \quad (27)$$

Formula (26) shows that a mean size of the ring is decreased as its deformation is increased. Of course, it is consistent with conservation of the total energy. The conservation law (27) is actually for z -component of the angular momentum. Excluding S_0 , we obtain an effective Hamiltonian of perturbations in the form

$$\begin{aligned} \tilde{H} = & \frac{m\sqrt{m^2-1}(|b_+|^2 + |b_-|^2)}{(2I - |b_+|^2 - |b_-|^2)} + \sqrt{2I - |b_+|^2 - |b_-|^2} \\ & - \epsilon \frac{\sqrt{m^2-1}}{4m} (b_+ b_- + b_+^* b_-^*) \\ & + T(|b_+|^4 + |b_-|^4) + W|b_+|^2 |b_-|^2. \end{aligned} \quad (28)$$

In terms of canonically conjugate variables $N = |b_+|^2 + |b_-|^2$ and $\Phi = [\arg(b_+) + \arg(b_-)]/2$ it is reduced to

$$\begin{aligned} \tilde{H} = & \frac{m\sqrt{m^2-1}N}{(2I - N)} - \epsilon \frac{\sqrt{m^2-1}}{4m} \sqrt{N^2 - D^2} \cos(2\Phi) \\ & + \sqrt{2I - N} + \frac{T}{2}(N^2 + D^2) + \frac{W}{4}(N^2 - D^2). \end{aligned} \quad (29)$$

The recurrence phenomenon then corresponds to quasi-closed phase trajectories in the complex plane of variable $C = \sqrt{(|A_+|^2 + |A_-|^2)/2} (A_+ A_-) / |A_+ A_-|$, as shown in Fig.2. Of course, the real phase trajectory only “in average” is described by the simplified model.

It is necessary also to say that applicability of the Hamiltonian (28) is limited by close-to-resonance values of the parameter I . Taking $2I = 4m^2(m^2 - 1) + \delta$

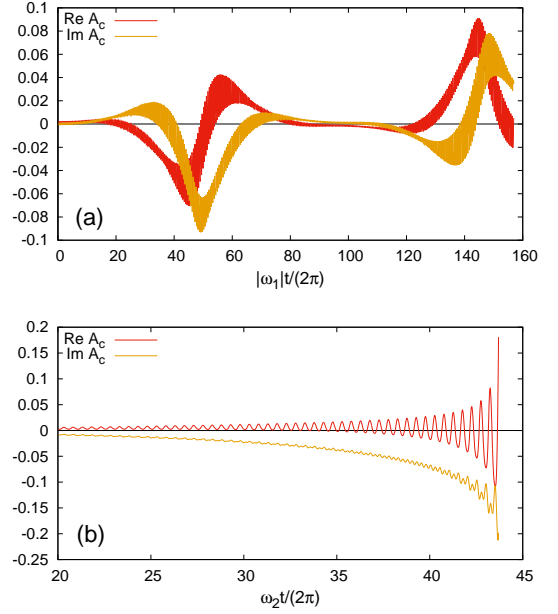


FIG. 3: Two types of nonlinear stage of parametric instabilities of a vortex ring in condensate with density $\rho = 1 - r^2 - \alpha z^2$, observed in numerical experiments. Shown are properly defined envelopes of unstable modes. The oscillations on the curves are caused by higher harmonics. In the first case $\alpha = 8/5$, $R(0) = 0.88/\sqrt{3} + 0.002 \cos(\varphi)$, $Z(0) = 0$. In the second case $\alpha = 16/7$, $R(0) = 0.95/\sqrt{3} + 0.002 \cos(2\varphi)$, $Z(0) = 0$.

and making expansion up to 4-th order on b_{\pm} , we obtain a quite simplified model Hamiltonian as written in Abstract. Its quadratic part corresponds to instability near the resonance.

Comparison to vortex ring in a harmonic trap.

Since we speak here about parametric instabilities of a quantum vortex ring, it makes sense to compare the above described instability mechanism to a situation where the condensate is bounded in space, and a finite motion of perfect circular ring is described by two periodic functions $R_0(t)$ and $Z_0(t)$. Specifically, we consider a density profile $\rho_h(z, r) = 1 - r^2 - \alpha z^2$ which is typical for harmonically trapped Bose-Einstein condensates in the Thomas-Fermi regime. Each phase trajectory of the perfect ring encompasses point $R_{\text{st}} = 1/\sqrt{3}$, $Z_{\text{st}} = 0$, while the squared eigenfrequencies of small oscillations are given by expression first obtained in Ref. [14]:

$$\omega_m^2 = 9(m^2 - 3)(m^2 - \alpha). \quad (30)$$

It follows from here that in the range $1 < \alpha < 4$ all the modes are linearly stable. In our approach this result is easily reproduced by introducing canonical variables $Q = 1 - R^2 - \alpha Z^2$ and $P = QZ/2$. The Hamiltonian of perfect ring is defined then by rather elegant expression,

$$\mathcal{H}_0 = \sqrt{Q_0^2 - 4\alpha P_0^2} - Q_0^3, \quad (31)$$

and the stationary point is $Q_{\text{st}} = 2/3$, $P_{\text{st}} = 0$. Let us study small deviations of ring from the equilibrium, by writing the local induction Hamiltonian $(2\pi)^{-1} \int \rho(Z, R) \sqrt{(R^2 + R'^2 + Z'^2)} d\varphi$ in terms of the new variables and expanding on powers of small functions $q = Q(\varphi, t) - 2/3$ and $p = P(\varphi, t)$. We thus obtain

$$\mathcal{H}^{\{2\}} = \sqrt{3} \sum_m \left[\frac{1}{4} (m^2 - 3) |q_m|^2 + 3(m^2 - \alpha) |p_m|^2 \right] \quad (32)$$

$$\mathcal{H}^{\{3\}} = -\frac{1}{2\pi} \int \left[\frac{3\sqrt{3}}{4} q^3 + \frac{9\sqrt{3}}{2} (\alpha - 1) p^2 q'' \right] d\varphi \quad (33)$$

The term $\mathcal{H}^{\{2\}}$ gives formula (30). In terms of normal complex variables defined as

$$a_m = \frac{(\sqrt{3}|m^2 - 3|/2)^{\frac{1}{2}} q_m + i(6\sqrt{3}|m^2 - \alpha|)^{\frac{1}{2}} p_m}{\sqrt{2|\omega_m|}}, \quad (34)$$

the quadratic Hamiltonian $\mathcal{H}^{\{2\}} = \sum_m \omega_m |a_m|^2$. It is very important that the two first frequencies ω_0 and ω_1 have the negative sign, while at $|m| \geq 2$ all ω_m are positive (which fact was not taken into account by the authors of Ref.[14], since they did not use the Hamiltonian method). Therefore at definite values of the anisotropy parameter α , nonlinear resonances arise between some modes, leading to parametric instabilities. In particular, the condition $\omega_0 \approx 2\omega_1$ takes place near $\alpha^{(1)} = 8/5$, and then nonlinear resonance processes occur which are described by interaction of the form $V^{(1)}(a_0^* a_1 a_{-1} + a_0 a_1^* a_{-1}^*)$, while at $\alpha \approx \alpha^{(2)} = 16/7$, when $\omega_0 \approx -2\omega_2$, in resonance are the processes corresponding to interaction in the form $V^{(2)}(a_0 a_2 a_{-2} + a_0^* a_2^* a_{-2}^*)$. In both situations, a weakly nonlinear dynamics is approximately described by integrable Hamiltonians of standard form:

$$\mathcal{H}^{(1)} = (\delta^{(1)} - 2\Omega^{(1)}) |a_0|^2 - \Omega^{(1)} (|a_1|^2 + |a_{-1}|^2) + V^{(1)}(a_0^* a_1 a_{-1} + a_0 a_1^* a_{-1}^*), \quad (35)$$

$$\mathcal{H}^{(2)} = (\delta^{(2)} - 2\Omega^{(2)}) |a_0|^2 + \Omega^{(2)} (|a_2|^2 + |a_{-2}|^2) + V^{(2)}(a_0 a_2 a_{-2} + a_0^* a_2^* a_{-2}^*), \quad (36)$$

where $\delta^{(1)}$ and $\delta^{(2)}$ are small frequency detuning parameters, and the coefficients $V^{(1)}$, $V^{(2)}$ can be calculated by re-writing $\mathcal{H}^{\{3\}}$ in terms of a_m . In the first case there are additional integrals of motion $|a_0|^2 + |a_1|^2 = s_+$ and $|a_0|^2 + |a_{-1}|^2 = s_-$, so the system remains in a weakly nonlinear regime, and a periodic recurrence of ring to an almost axisymmetric state occurs, as it is shown in Fig.3a. In the second case, the additional integrals of motion are $|a_0|^2 - |a_2|^2 = d_+$ and $|a_0|^2 - |a_{-2}|^2 = d_-$, and the parametric instability has an explosive character, as it is seen in Fig.3b. In fact, as numerical simulations of system (3)-(4) at $\rho = 1 - r^2 - \alpha z^2$ demonstrate, at the final stage of the explosive instability so large deformation of the vortex ring is attained that some its parts closely approach the Thomas-Fermi surface (which is an effective condensate boundary), and there the hydrodynamic anelastic approximation certainly fails.

Conclusions. Thus, in this work for the first time we have predicted the parametric instability of oscillations of quantum vortex ring in a spatially periodic Bose-Einstein condensate at definite sizes of the ring, and also in harmonically trapped condensate — at definite values of the trap anisotropy. In all the cases, we numerically simulated nonlinear stages of the instabilities. The found here phenomenon of quasi-recurrence was theoretically explained. Such kind nontrivial behaviour of vortex ring definitely deserves further studies within more accurate models. In particular, it is very desirable to reproduce the parametric instability at moderate values of Λ immediately in a numerical solution of the 3D Gross-Pitaevskii equation with periodic external potential, as well as in anisotropic harmonic potential. After that, organization of some real-world experiments could become actual.

-
- [1] A. L. Fetter, Rev. Mod. Phys. **81**, 647 (2009).
[2] A. A. Svidzinsky and A. L. Fetter, Phys. Rev. A **62**, 063617 (2000).
[3] A. L. Fetter and A. A. Svidzinsky, J. Phys.: Condens. Matter **13**, R135 (2001).
[4] V. P. Ruban, Phys. Rev. E **64**, 036305 (2001).
[5] A. Aftalion and T. Riviere, Phys. Rev. A **64**, 043611 (2001).
[6] J. Garcia-Ripoll and V. Perez-Garcia, Phys. Rev. A **64**, 053611 (2001).
[7] J. R. Anglin, Phys. Rev. A **65**, 063611 (2002).
[8] P. Rosenbusch, V. Bretin, and J. Dalibard, Phys. Rev. Lett. **89**, 200403 (2002).
[9] A. Aftalion and I. Danaila, Phys. Rev. A **68**, 023603 (2003).
[10] A. Aftalion and I. Danaila, Phys. Rev. A **69**, 033608 (2004).
[11] D. E. Sheehy and L. Radzihovsky, Phys. Rev. A **70**, 063620 (2004).
[12] I. Danaila, Phys. Rev. A **72**, 013605 (2005).
[13] A. Fetter, Phys. Rev. A **69**, 043617 (2004).
[14] T.-L. Horng, S.-C. Gou, and T.-C. Lin, Phys. Rev. A **74**, 041603 (2006).
[15] S. Serafini, L. Galantucci, E. Iseni, T. Bienaime, R. N. Bisset, C. F. Barenghi, F. Dalfovo, G. Lamporesi, G. Ferrari, Phys. Rev. X **7**, 021031 (2017).
[16] R. N. Bisset, S. Serafini, E. Iseni, M. Barbiero, T. Bienaime, G. Lamporesi, G. Ferrari, F. Dalfovo, [arXiv:1705.09102](https://arxiv.org/abs/1705.09102).
[17] V. P. Ruban, JETP Letters **105**, 458 (2017).
[18] V. P. Ruban, JETP **124**, 932 (2017); [arXiv:1612.00165](https://arxiv.org/abs/1612.00165).
[19] H. Hasimoto, J. Fluid Mech. **51**, 477 (1972).
[20] V. P. Ruban, JETP Letters **103**, 780 (2016).
[21] V. P. Ruban, JETP Letters **104**, 868 (2016).